

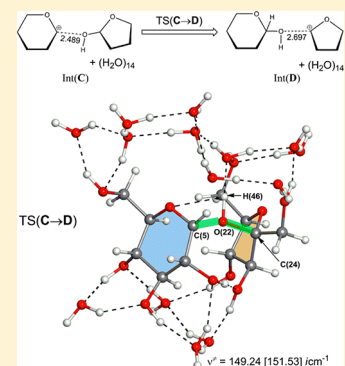
Three Competitive Transition States at the Glycosidic Bond of Sucrose in Its Acid-Catalyzed Hydrolysis

Shinichi Yamabe,* Wei Guan, and Shigeyoshi Sakaki

Fukui Institute for Fundamental Chemistry, Kyoto University, Takano-Nishihiraki-cho 34-4, Kyoto, Japan

S Supporting Information

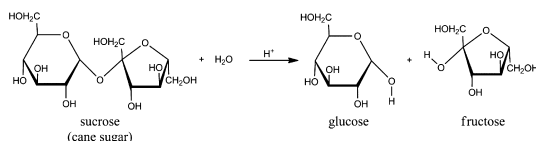
ABSTRACT: The acid-catalyzed hydrolysis of sucrose to glucose and fructose was investigated by DFT calculations. Protonations to three ether oxygen atoms of the sucrose molecule, A, B, and (C, D), were compared. Three (B, the fructosyl-ring oxygen protonation; C, protonation to the bridge oxygen of the glycosidic bond for the glucosyl-oxygen cleavage; and D, protonation to that for the fructosyl-oxygen cleavage) gave the fragmentation. Paths B, C, and D were examined by the use of the sucrose molecule and $\text{H}_3\text{O}^+(\text{H}_2\text{O})_{13}$. The path B needs a large activation energy, indicating that it is unlikely. The fragmentation transition state (TS1) of path C needs almost the same activation energy as that of path D. The isomerization TS of $\text{Int}(\text{C}) \rightarrow \text{Int}(\text{D})$, $\text{TS}(\text{C} \rightarrow \text{D})$, was also obtained as a bypass route. The present calculations showed that the path via the fructosyl-oxygen cleavage (D) is slightly (not absolutely) more favorable than that via the glucosyl-oxygen cleavage (C).



1. INTRODUCTION

The acid-catalyzed hydrolysis of sucrose has a long history (Scheme 1). It would be the first catalytic reaction that was

Scheme 1. Acid-Catalyzed Hydrolysis of Sucrose

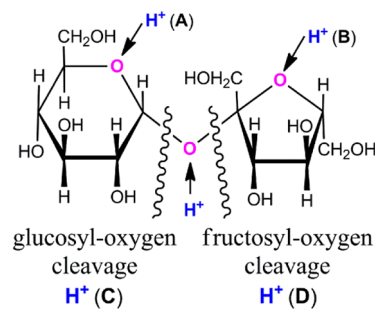


observed in 1806,¹ and Arrhenius developed his equation using data from the sucrose hydrolysis measurement.² By the acid catalyst, the site of protonation is generally considered to be the bridge oxygen of the glycosidic bond (the central ether bond), although protonation of the fructosyl-ring oxygen [$\text{H}^+(\text{B})$ in Scheme 2] has also been proposed.³

The question of the site of bond cleavage caused by the protonation seems to remain unsettled probably because of difficulties in NMR measurements. BeMiller suggested that a scheme involving fructosyl-oxygen bond cleavage [$\text{H}^+(\text{D})$ in Scheme 2] was likely but commented that “more experiments need to be done”⁴

By kinetic analyses, the fructosyl-oxygen cleavage was suggested.⁵ On the other hand, “Transition of the protonated form from the chair to half-chair conformation with a cyclic carbonium ion is the rate-determining step of pyranoside hydrolysis.”⁶ This suggested solely the glucosyl-oxygen cleavage [$\text{H}^+(\text{C})$ in Scheme 2]. Also, the glucosyl-oxygen cleavage was shown as a mechanism of the hydrolysis.⁷ In a text book, a detailed reaction mechanism involving the glucosyl-oxygen bond fission was explained.⁸ Through an ^{18}O -labeling study, both fructosyl-oxygen and glucosyl-oxygen scission were suggested to occur.⁹ A study of

Scheme 2. Four Possible Protonations, A, B, C and D, to Three Ether Oxygen Atoms Contained in the Sucrose Molecule

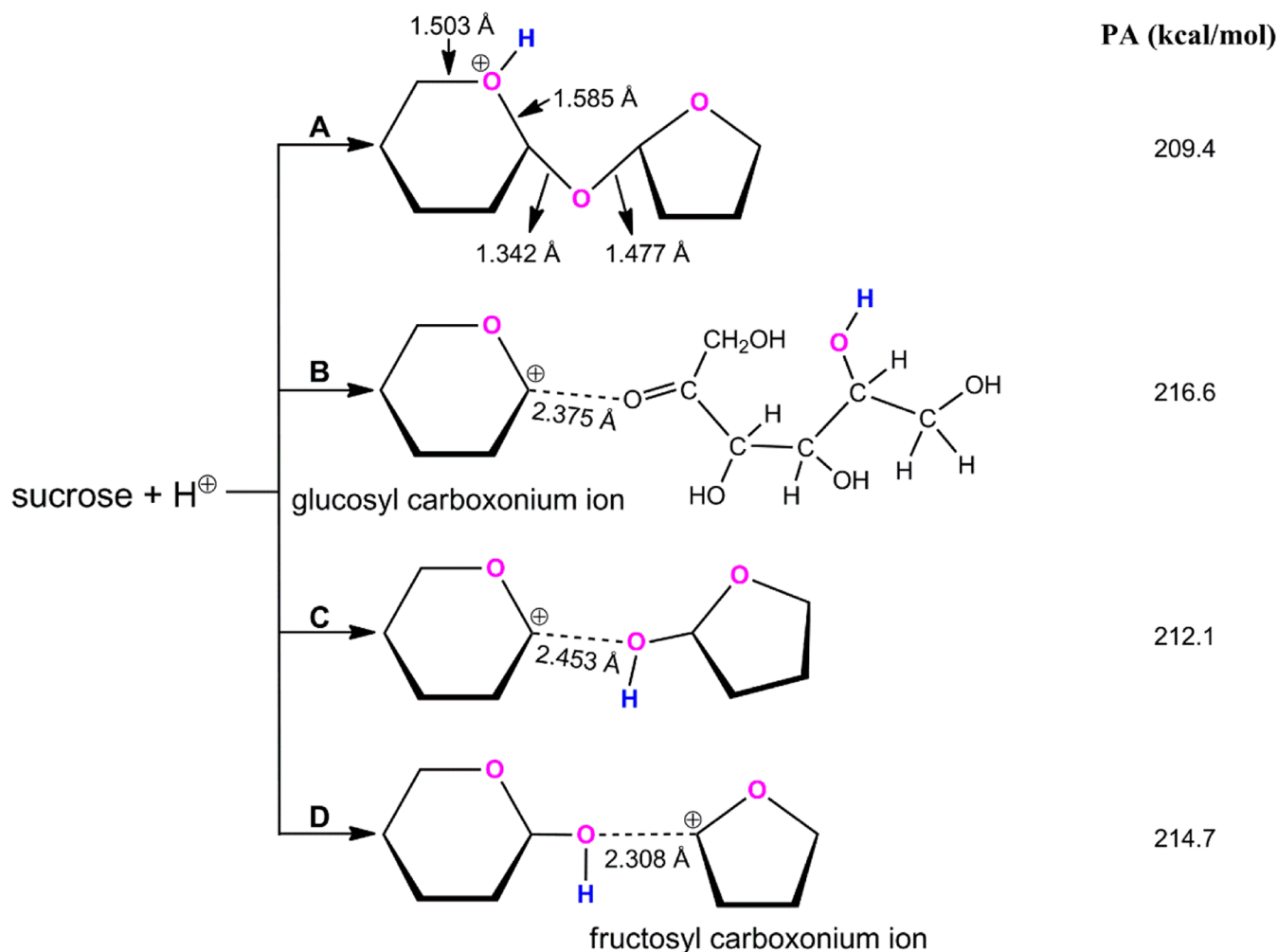


oligosaccharide formation in beet medium invert sugar^{10a} and an analysis of three disaccharides from a total invert sugar^{10b} have been reported. Both studies suggested that the acid-catalyzed hydrolysis of sucrose involves initial protonation of the glycosidic oxygen, leading to the formation of either glucopyranosyl or fructofuranosyl oxonium ion and D-fructose or D-glucose, respectively. A study of the ^{18}O isotope shift in ^{13}C NMR spectroscopy indicated the fructosyl-oxygen cleavage.¹¹ As for the carbocation intermediate formed by the protonation, a five-membered ring tertiary carboxonium ion would be more stable than a six-membered ring secondary carboxonium ion.¹²

Although the acid-catalyzed hydrolysis of sucrose is a familiar and classic reaction, surprisingly there have been no theoretical studies on its mechanism. Hydrogen bonds promoting proton transfers need to be considered explicitly. As the first attempt, in this work, the reaction paths of the hydrolysis were investigated by DFT calculations. Since “elucidation of subtle mechanistic

Received: December 19, 2012

Published: February 1, 2013

Scheme 3. Protonations of Three Ether (C–O–C) Oxygen Atoms of Sucrose According to Scheme 2^a

^aBoth paths C and D begin with the protonation of the same O atom, and protonation of the fructose O (path B) leads via an energetically downhill path to the spontaneous breakup of the five-membered ring. Proton affinity (PA) was calculated by the difference of B3LYP/6-311G(d,p) electronic and zero-point vibrational energies. Geometric data are given by Cartesian coordinates in Supporting Information.

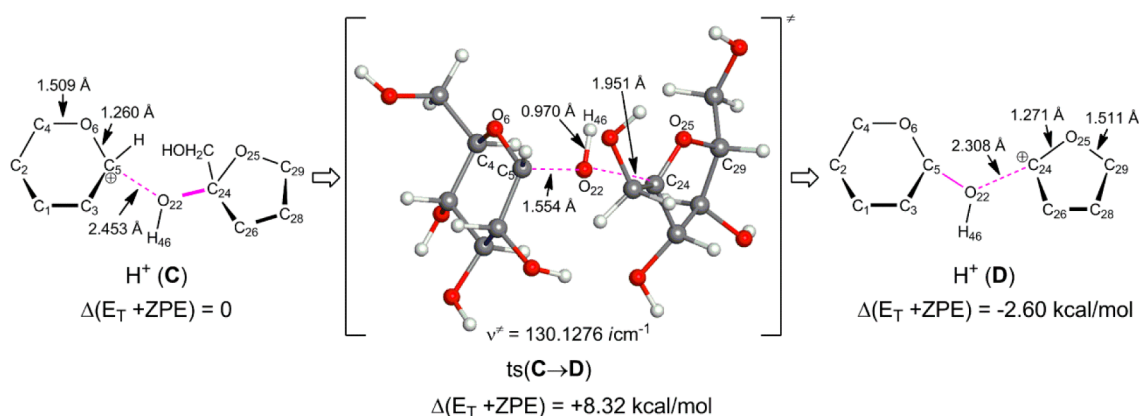


Figure 1. An isomerization reaction from the (glucosyl carboxonium ion... β -D-fructofuranose) complex to the (α -D-glucopyranose...fructosyl carboxonium ion) one.

details, such as the site(s) of protonation, is essential for the bond cleavage¹¹, geometric isomers of the protonated sucrose were examined in section 3.1. In section 3.2, reaction paths were traced by the use of a system composed of sucrose and H₃O⁺(H₂O)₁₃.

2. METHOD OF CALCULATION

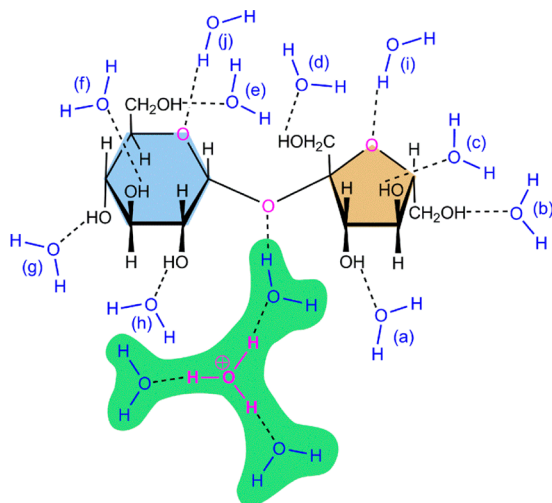
The reacting systems were investigated by density functional theory calculations. The B3LYP¹³ method was used. As examples of the excellent performance of B3LYP, for the 622 compounds containing C, H, O, and N atoms, the mean absolute errors in the heats of formation

were reported to be a few kcal/mol with various basis sets.^{14a} B3LYP was found to be the most reliable method for studying small zeolite clusters among various DFT functionals.^{14b} The basis set employed here was 6-311G(d,p), because the present systems are large (for molecular formula $C_{12}H_{51}O_{25}^+$, 1009 basis functions are used in the geometry optimizations), and calculations by a higher-level basis set than 6-311G(d,p) are too difficult. Transition states (ts and TSs) were sought first by partial optimizations at bond interchange regions. Second, by the use of Hessian matrices TS geometries were optimized. They were characterized by vibrational analyses, which checked whether the obtained geometries have single imaginary frequency (ν^+). From TSs, reaction paths were traced by the intrinsic reaction coordinate (IRC) method¹⁵ to obtain the energy-minimum geometries. Similar geometry optimizations and subsequent vibrational analyses were carried out including the PCM¹⁶ solvation effect, B3LYP/6-311G(d,p) SCRF = (PCM, solvent = water) opt freq. All calculations were carried out with the GAUSSIAN 09¹⁷ program package. The computations were performed at the Research Center for Computational Science, Okazaki, Japan.

3. RESULTS AND DISCUSSION

1. Protonation of the Sucrose Molecule. The sucrose molecule has three ether oxygen atoms that may be subject to the protonation. Their positions are shown in Scheme 2 as A, B, and (C, D). Geometries of the protonated sucrose were optimized, as shown in Scheme 3.

Scheme 4. An Assumed Model of Sucrose and $H_3O^+(H_2O)_3$ for Geometry Optimizations for C and D in Scheme 2^a



^aFor B, the position of the $H_3O^+(H_2O)_3$ group in the green area and that of $H_2O(i)$ are switched. In geometric figures, hereafter, the glucosyl six-membered ring is shown by the blue color and the fructosyl five-membered one by the yellowish-brown one, respectively. Larger models than sucrose and $H_3O^+(H_2O)_3$ met technical difficulties in TS searches.

The protonation A was found not to give fragmentation to glucosyl and fructosyl moieties. In addition, $PA(A)$ (= +209.4 kcal/mol) is the smallest one among the four (the most unfavorable protonation). Thus, protonation A is ruled out for the further investigation. The protonation B gives the fragmentation with the largest value of $PA(B)$ (= +216.6 kcal/mol). The reaction channel corresponding to protonation B needs to be examined in line with the experimental suggestion.³ Protonation to the oxygen of the glycosidic bond gives isomers C and D.

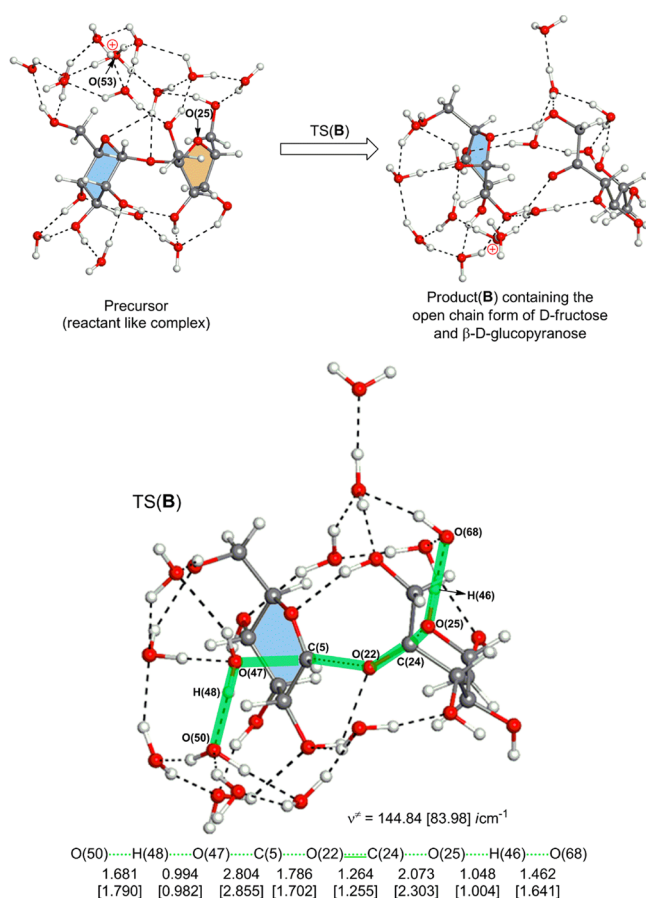


Figure 2. Geometry changes of B3LYP/6-311G(d,p) along the protonation B path (Schemes 2 and 3). Bond interchange regions are marked by green colors, and distances are shown in Å. In square brackets, B3LYP/6-311G(d,p) SCRF = PCM data are shown. Very small energy first derivatives could not be eliminated despite over 500 cycles of the geometry optimization of TS(B) by B3LYP/6-311G(d,p) SCRF = PCM. Numerical details (Cartesian coordinates and various energies) are shown in Supporting Information.

Their PA values are similar (212.1 and 214.7 kcal/mol). The distances between the carbocation and the hydroxyl oxygen is small, 2.453 (C) and 2.308 (D) Å. An isomerization path between C and D is expected, and in fact the transition state (ts) was obtained. It is exhibited in Figure 1 with the OH^- shift TS between two carboxonium ions. The calculated activation energy is small (= +8.32 kcal/mol) and the isomerization readily takes place.

In view of the results of the sucrose protonation, three reaction channels corresponding to B, C and D need to be investigated. In addition, a transformation between C and D might be involved in the hydrolysis path.

2. Search for Hydrolysis Paths. Scheme 4 shows a model composed of the sucrose molecule and $H_3O^+(H_2O)_3$ for tracing reaction paths. Here, eight water molecules, $H_2O(a)$, $H_2O(b)$, ..., $H_2O(h)$, are linked to eight H–O groups of sucrose, respectively. To three ether oxygen atoms, H–OH(i), H–OH(j), and H–O(H) $H_3O^+(H_2O)_2$ in the green area are attached, respectively. First, a path corresponding to the protonation B was sought, and the calculated results are shown in Figure 2. In line with the model in Scheme 4, the hydronium ion [$H_3O(53)^+$] in the precursor geometry is not directly linked with the ether oxygen O(25) of the fructosyl ring.

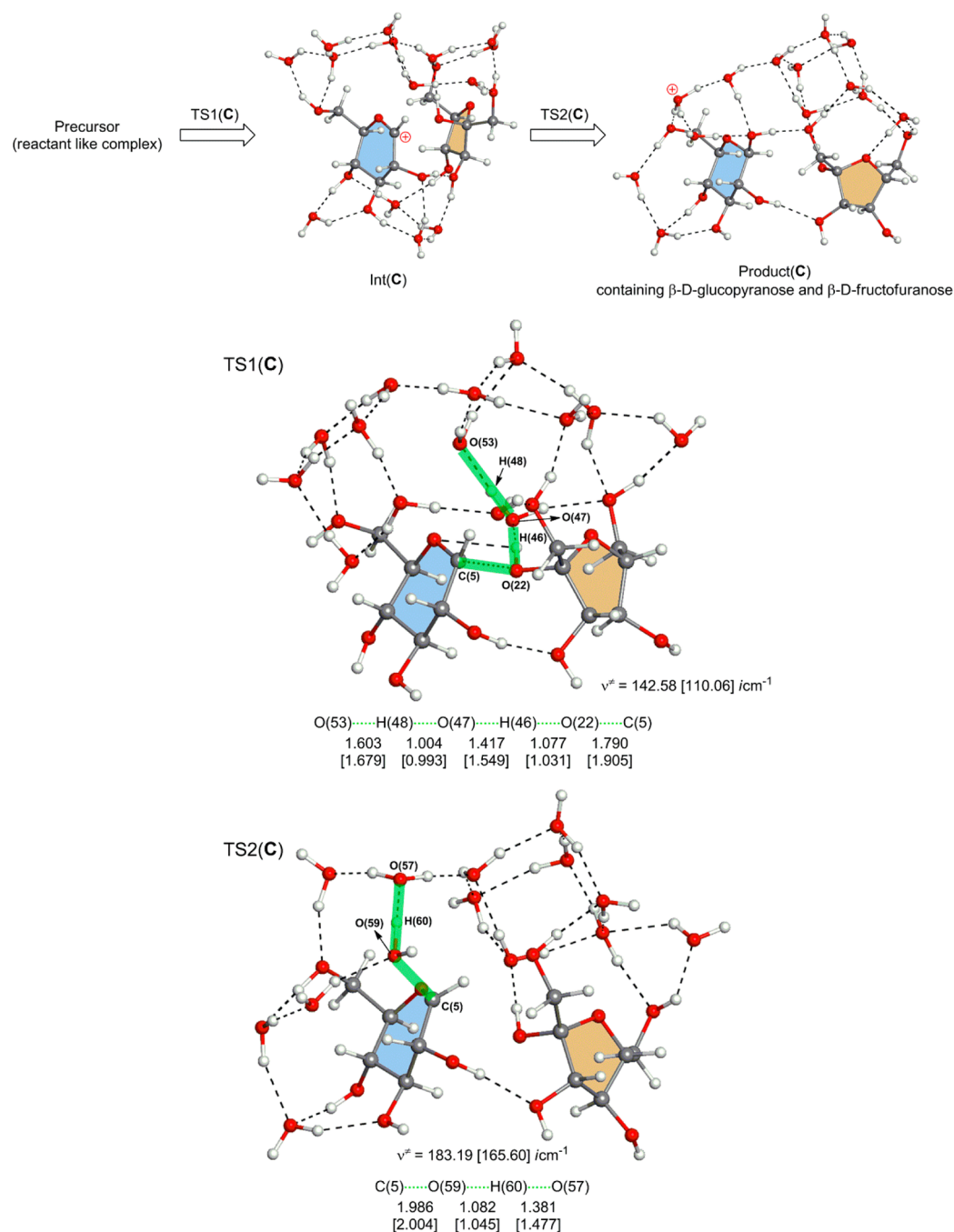
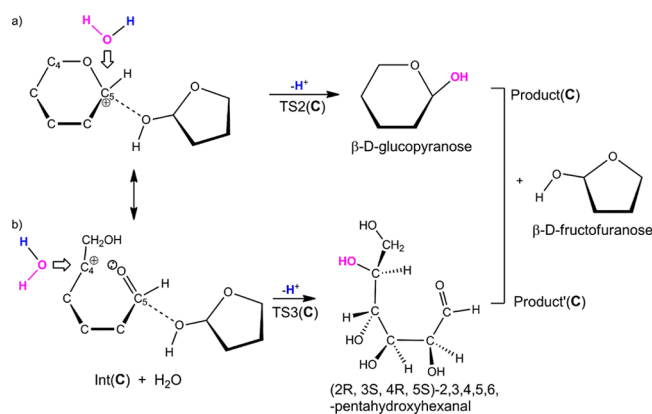


Figure 3. Geometric changes along the protonation C path (glucosyl-oxygen cleavage).

From the precursor, the geometry of TS(B) was obtained. At TS(B), O(68)–H(46), O(25)–C(24), O(22)–C(5), and O(47)–H(48) covalent bonds are broken. The O(25)–H(46) and C(5)–O(47) bonds are newly formed, and the C(24)–O(22) becomes a carbonyl group. These bond interchanges take place simultaneously. That is to say, TS(B) is of the concerted path (without the carboxonium-cation intermediate) leading to the open chain form of D-fructose and β (not α)-D-glucopyranose in product(B). The concerted function arises from the condition that the C(5)···O(22) bond cleavage is not directly linked with the protonation and the assistance of the S_N2 type O(47)···C(5)···O(22) push–pull bond interchange is required. Thus, the channel for protonation B was found.

Figure 3 shows the reaction path including the glucosyl-oxygen cleavage. At TS1(C), the simultaneous bond interchange of O(53)···H(48)···O(47)···H(46)···O(22)···C(5) is involved. After TS1(C), the intermediate Int(C) including the glucosyl carboxonium ion and fructose is formed. The subsequent nucleophilic attack of H₂O to the carbocation C(5) takes place at the back side in TS2(C). The attack leads to the formation of product(C) composed of β -D-glucopyranose and β -D-fructofuranose.

The cation in Int(C) has two canonical resonance structures as exhibited in the left side of Scheme 5. If C(4) is more positively charged than C(5) in Int(C), the S_N2-type in-plane channel b would be as likely as the out-of-plane one, TS2(C) in pathway a. However, in pathway b, the back-side attack produces the product (2R,3S,4R,5S)-2,3,4,5,6-pentahydroxyhexanal, which is different

Scheme 5. Two Paths of the H₂O Nucleophilic Attack to the Glucosyl Carboxonium Ion in Int(C) of Figure 3


from the open form of D-glucose with the (2R,3S,4R,5R) configuration. In fact, in H⁺(C) (Int(C) without water molecules, in Figure 1) the Mulliken atomic charges are +0.26 on C(5) and -0.01 on C(4). Accordingly, the activation energy of the in-plane S_N2 step in path b, TS3(C), is much larger than that of TS2(C), which will be shown in Figure 6. Thus, path b is ruled out, and the channel for the protonation C is, Precursor → TS1(C) → Int(C) → TS2(C) → Product (β-cyclic forms of glucose and fructose).

Figure 4 exhibits the path for the fructosyl-oxygen cleavage. At TS1(D), the bond interchange occurs in the O(53)⋯H(48)⋯O(47)⋯H(46)⋯O(22)⋯C(24) moiety. After TS1(D), Int(D) composed of the fructosyl carboxonium ion and glucose is afforded. Through the process Int(D) → TS2(D) → product(D), the pair of α-D-glucopyranose and α-D-fructofuranose is formed.

Figure 5 show the TS geometry of the isomerization between Int(C) and Int(D), which corresponds to the gas-phase reaction

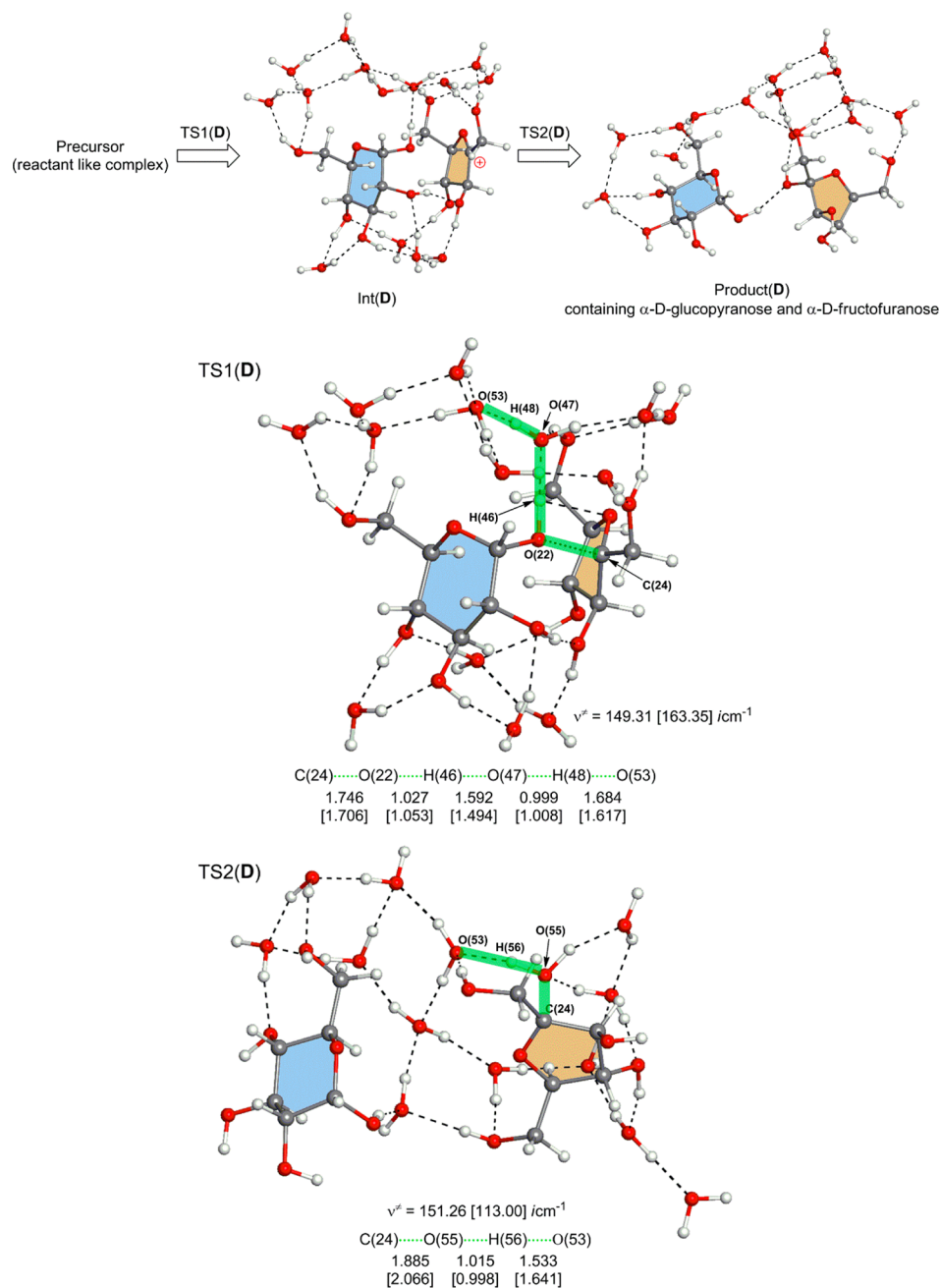


Figure 4. Geometric changes along the protonation D path (fructosyl-oxygen cleavage).

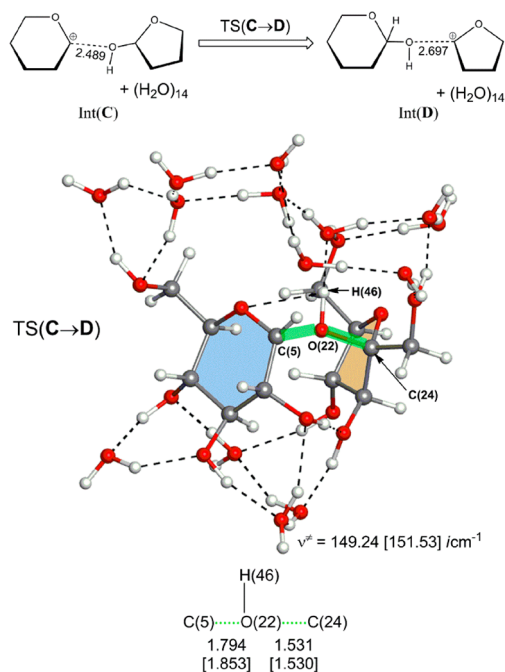


Figure 5. An isomerization reaction similar to that in Figure 1. Geometries of Int(C) and Int(D) are shown in Figures 3 and 4, respectively.

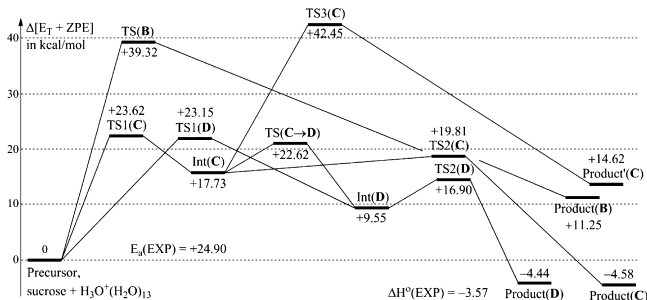


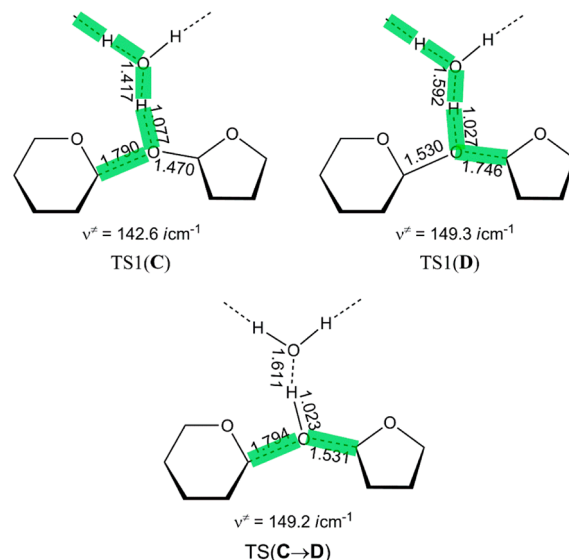
Figure 6. Energy changes (kcal/mol) of B3LYP/6-311G(d,p) SCRFF = PCM optimized geometries in three reaction channels, B, C and D. $\Delta[E_T + ZPE]$ is the difference of electronic and zero-point vibrational energies. TS3(C) and Product(C) are defined in Scheme 5. Experimental energies, $E_a(\text{EXP})$ and $\Delta H^\circ(\text{EXP})$, are taken from refs 19 and 20, respectively.

in Figure 1. While the TS(C \rightarrow D) geometry is similar to that of TS1(C), IRC calculations gave different paths, isomerization of cations and decomposition to the monosaccharide moieties, respectively. If the isomerization occurs easily, its path is for the acid-catalyzed mutarotation between α and β anomeric forms.¹⁸

3. Energy Changes along the Calculated Paths. Figure 6 exhibits the energies of B3LYP/6-311G(d,p) SCRFF = PCM. TS(B) needs an activation energy (+39.32 kcal/mol) much larger than those of TS1(C) and TS1(D). The channel of the protonation to the fructosyl-ring oxygen³ was calculated to be unlikely.

Energies of TS1(C) and TS1(D) are larger than those of TS2(C) and TS2(D), respectively. This result indicates that either the glycosyl-oxygen cleavage or the fructosyl-ring oxygen one is the rate-determining step. Noteworthy is the very small difference of activation energies between TS1(C) (= +23.62 kcal/mol) and TS1(D) (= +23.15 kcal/mol). While TS1(D) is only slightly more favorable than TS1(C), Int(D) is more stable than Int(C). Therefore, even if both intermediates Int(C) and

Scheme 6. Three Similar but Distinguishable Transition States at the Glycosidic Bond with Main Distances in Å^a



^aTS1(C), TS1(D), and TS(C \rightarrow D) are shown in Figures 3, 4 and 5, respectively.

Int(D) are formed kinetically and transiently, Int(C) is converted to Int(D) through TS(C \rightarrow D) for the isomerization. In fact, the activation energy of this TS (= +22.62 kcal/mol) is slightly smaller than those of TS1(C) and TS1(D). The superiority of the fructosyl-ring oxygen cleavage over the glucosyl-ring oxygen one is attained thermodynamically via the bypass channel, TS(C \rightarrow D). Three calculated activation energies, +23.62 kcal/mol of TS1(C), +23.15 of TS1(D), and 22.62 of TS(C \rightarrow D), are in good agreement with experimental E_a value $E_a(\text{EXP}) = +24.90$ kcal/mol. Also, reaction energies, -4.44 of Product(D) and -4.58 of Product(C), are close to $\Delta H^\circ(\text{EXP}) = -3.57$ kcal/mol.

4. CONCLUSION

In this work, reaction paths of the acid-catalyzed hydrolysis of sucrose were investigated by DFT calculations. First, protonations to three ether oxygen atoms of the sucrose molecule, A, B, and (C, D) were examined. B, C, and D protonated species contain the monosaccharide moieties. In C and D species, the C \cdots O coordination bond is relatively strong, and their isomerization TS, ts(C \rightarrow D), was obtained.

Second, by the use of the sucrose and $\text{H}_3\text{O}^+(\text{H}_2\text{O})_{13}$ model, B, C, and D paths of the acid-catalyzed hydrolysis were traced. The path B affording β -glucose and the open form of D-fructose was calculated to be unlikely owing to the large activation energy of TS(B). TS1(C) leading to the β forms of glucose and fructose was found to have almost the same activation energy as that of TS(D) leading to α forms. On the other hand, Int(D) is more stable than Int(C). The isomerization path of Int(C) \rightarrow Int(D) was also obtained.

The present calculations show that the fructosyl-oxygen bond cleavage is slightly more favorable than the glucosyl-oxygen one, not kinetically but thermodynamically. In other words, while both cleavages (C and D) occur primarily, the subsequent Int(C) \rightarrow Int(D) isomerization takes place concomitantly. The present scheme is close to the mechanism suggested by Low and co-workers.¹⁰ In conclusion, there are three competitive TS

structures, TS1(C), TS1(D), and TS(C→D) at the bridge oxygen of the glycosidic bond, which are shown in Scheme 6.

■ ASSOCIATED CONTENT

■ Supporting Information

The neutral reaction path [I] of the mutarotation of glucose with $(\text{H}_2\text{O})_9$, the H^+ containing reaction path [II] with $\text{H}_3\text{O}^+(\text{H}_2\text{O})_8$, and Cartesian coordinates of all the optimized geometries. This material is available free of charge via the Internet at <http://pubs.acs.org>.

■ AUTHOR INFORMATION

Corresponding Author

*E-mail: yamabes@fukui.kyoto-u.ac.jp.

Notes

The authors declare no competing financial interest.

■ ACKNOWLEDGMENTS

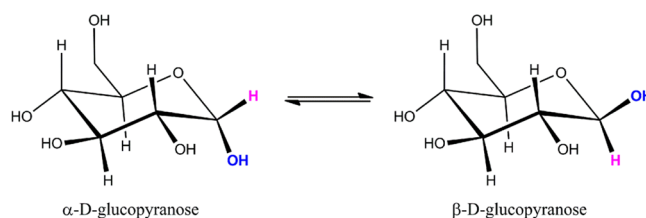
This work is financially supported by the Grants-in-Aid from Ministry of Education, Culture, Science, Sport, and Technology through Grants-in-Aid of Specially Promoted Science and Technology (No. 22000009) and Grand Challenge Project (IMS, Okazaki, Japan). We are also thankful to the computational facility at the Institute of Molecular Science, Okazaki, Japan.

■ REFERENCES

- (1) Clement, N.; Desormes, C.-B. *Ann. Chim. Phys.* **1806**, 59, 329–339.
- (2) Arrhenius, S. *Z. Phys. Chem. (Leipzig)* **1889**, 4, 226–248.
- (3) Szejtli, J.; Henriques, R. D.; Castifeira, M. *Acta Chim. Acad. Sci. Hung.* **1970**, 66, 213–227.
- (4) BeMiller, J. N. *Adv. Carbohydr. Chem.* **1967**, 22, 25–108.
- (5) Barnett, J. W.; O'Conner, C. *J. Chem. Soc. B* **1971**, 1163–1165.
- (6) Moiseev, Y. V.; Khalturinskii, N. A.; Zaikov, G. E. *Carbohydr. Res.* **1976**, 51, 23–37.
- (7) Dawber, J. G.; Brown, D. R.; Reed, R. A. *J. Chem. Educ.* **1966**, 43, 34–35.
- (8) Bender, M. L.; Brubacher, L. J. *Catalysis and Enzyme Action*; McGraw-Hill: New York, 1973; pp 40–43.
- (9) Eisenberg, F. *Carbohydr. Res.* **1969**, 11, 521–530.
- (10) (a) Swallow, K. W.; Low, N. H. *J. Agric. Food Chem.* **1993**, 41, 1587–1592. (b) Thavarajah, P.; Low, N. H. *J. Agric. Food Chem.* **2006**, 54, 2754–2760.
- (11) Mega, T. L.; Van Etten, R. L. *J. Am. Chem. Soc.* **1988**, 110, 6372–6376.
- (12) Capon, B. *Chem. Rev.* **1969**, 69, 407–498.
- (13) (a) Becke, A. D. *J. Chem. Phys.* **1993**, 98, 5648–5652. (b) Lee, C.; Yang, W.; Parr, R. G. *Phys. Rev. B* **1988**, 37, 785–789.
- (14) (a) Tirado-Rives, J.; Jorgensen, W. L. *J. Chem. Theory Comput.* **2008**, 4, 297–306. (b) Zygmunt, S. A.; Mueller, R. M.; Curtiss, L. A.; Iton, L. E. *J. Mol. Struct. (THEOCHEM)* **1998**, 430, 9–16.
- (15) (a) Fukui, K. *J. Phys. Chem.* **1970**, 74, 4161–4163. (b) Gonzalez, C.; Schlegel, H. B. *J. Chem. Phys.* **1989**, 90, 2154–2161.
- (16) (a) Cances, E.; Mennucci, B.; Tomasi, J. *J. Chem. Phys.* **1997**, 107, 3032–3041. (b) Cossi, M.; Barone, V.; Mennucci, B.; Tomasi, J. *Chem. Phys. Lett.* **1998**, 286, 253–260. (c) Mennucci, B.; Tomasi, J. *J. Chem. Phys.* **1997**, 106, 5151–5158.
- (17) Frisch, M. J.; Trucks, G. W.; Schlegel, H. B.; Scuseria, G. E.; Robb, M. A.; Cheeseman, J. R.; Scalmani, G.; Barone, V.; Mennucci, B.; Petersson, G. A.; Nakatsuji, H.; Caricato, M.; Li, X.; Hratchian, H. P.; Izmaylov, A. F.; Bloino, J.; Zheng, G.; Sonnenberg, J. L.; Hada, M.; Ehara, M.; Toyota, K.; Fukuda, R.; Hasegawa, J.; Ishida, M.; Nakajima, T.; Honda, Y.; Kitao, O.; Nakai, H.; Vreven, T.; Montgomery, Jr., J. A.; Peralta, J. E.; Ogliaro, F.; Bearpark, M.; Heyd, J. J.; Brothers, E.; Kudin, K. N.; Staroverov, V. N.; Kobayashi, R.; Normand, J.; Raghavachari, K.; Rendell, A.; Burant, J. C.; Iyengar, S. S.; Tomasi, J.; Cossi, M.; Rega, N.;

Millam, N. J.; Klene, M.; Knox, J. E.; Cross, J. B.; Bakken, V.; Adamo, C.; Jaramillo, J.; Gomperts, R.; Stratmann, R. E.; Yazyev, O.; Austin, A. J.; Cammi, R.; Pomelli, C.; Ochterski, J. W.; Martin, R. L.; Morokuma, K.; Zakrzewski, V. G.; Voth, G. A.; Salvador, P.; Dannenberg, J. J.; Dapprich, S.; Daniels, A. D.; Farkas, O.; Foresman, J. B.; Ortiz, J. V.; Cioslowski, J.; Fox, D. J. *Gaussian 09, Revision B.01*; Gaussian, Inc.: Wallingford, CT, 2010.

(18) The mutarotation of glucose and fructose is known to occur readily in aqueous solution. Its reaction path of glucose including three^{18a} or one^{18b} water molecules was traced by DFT calculations. (a) Yamabe, S.; Ishikawa, T. *J. Org. Chem.* **1999**, 64, 4519–4524. (b) Lewis, B. E.; Choytun, N.; Schramm, V. L.; Bennett, A. J. *J. Am. Chem. Soc.* **2006**, 128, 5049–5058. Here, by the use of a model of glucose + $(\text{H}_2\text{O})_9$, [I] and glucose + $\text{H}_3\text{O}^+(\text{H}_2\text{O})_8$, [II], the effect of the acid catalyst on the mutarotation was investigated. The path [I] is shown in Figure S1 and [II] in Figure S2 in Supporting Information, respectively. When their activation energies are compared, the path [II] was found to be more favorable than [I]. Thus, the acid-catalyzed hydrolysis of sucrose (with the largest $E_a = +23.62$ kcal/mol in likely paths) inevitably undergoes the mutarotation of glucose (with the largest $E_a = +13.00$ kcal/mol) and probably fructose.



(19) Moelwyn-Hughes, E. A. *Kinetics of Reaction in Solution*, 2nd ed.; Clarendon Press: Oxford, 1947; chapters 1 and 2.

(20) Goldberg, R. N.; Tewari, Y. B.; Ahlumalia, J. C. *J. Biol. Chem.* **1989**, 264, 9901–9904.